LABORATORY INVESTIGATION - HUMAN/ANIMAL TISSUE

The feasibility of real-time in vivo optical detection of blood–brain barrier disruption with indocyanine green

Aysegul Ergin · Mei Wang · Jane Y. Zhang ·
Jeffrey N. Bruce · Robert L. Fine · Irving J. Bigio ·
Shailendra Joshi

Abstract Osmotic disruption of the blood–brain barrier (BBB) by intraarterial mannitol injection is sometimes required for the delivery of chemotherapeutic drugs to brain tissue. Osmotic disruption is affected by a number of factors, and there is a significant variability in the degree and distribution of BBB disruption in clinical and experimental settings. Brain tissue concentrations of indocyanine green (ICG) can be measured by optical techniques. The aim of this experiment was to determine whether the disruption of the BBB significantly altered the regional pharmacokinetics of ICG. We were able to track in vivo brain tissue concentrations of ICG in 13 New Zealand white rabbits by employing a novel optical approach. Evan's blue was used to assess the distribution of BBB disruption on post mortem examination. BBB disruption by intraarterial mannitol injection was found to be highly variable, and only five of the 13 animals demonstrated the disruption at the site of optical measurements. In these animals, we observed a ninefold increase in ICG concentrations and fourfold increase in the area under the concentration-time curve, compared to those without BBB disruption at the site of measurement. This study shows the feasibility of optical monitoring of BBB disruption with intravenous (IV) ICG injections. Virtual real-time optical monitoring of the BBB disruption could help improve intraarterial delivery of chemotherapeutic drugs.

Keywords Blood–brain barrier disruption · Indocyanine green · Intraarterial mannitol · Optical pharmacokinetics

Introduction

Indocyanine green (ICG) is a water soluble tricarbocyanine dye that is widely used for ophthalmic angiography [1] and in physiological studies such as, the measurement of cardiac output [2] or hepatic blood flow [3]. It has recently been introduced for intra-operative angiography during neurovascular surgery [3]. Concentrations of ICG in the human brain tissue can be determined in vivo by using near infrared spectroscopy (NIRS), and such measurements have been used for the determination of cerebral blood flow (CBF) [4, 5]. It is generally assumed that there is little or no retention of IGC by the cerebral tissue in these measurements. While this may be true in physiological states where the BBB is intact, there are relatively few investigations into ICG uptake by the brain tissue following disruption of the blood–brain barrier. If the brain tissue retains detectable quantities of ICG following BBB disruption, then ICG could used for detecting, and perhaps even quantifying, the degree of disruption. The disruption of the BBB is sometimes considered to be a critical step in the delivery of chemotherapeutic drugs and is currently

A. Ergin · J. Y. Zhang · I. J. Bigio
Department of Biomedical Engineering, Boston University, Boston, MA 02215, USA

M. Wang · S. Joshi (✉)
Department of Anesthesiology, College of Physicians and Surgeons of Columbia University, 630 West 168th Street, P&S P Box 46, New York, NY 10032, USA
e-mail: sj121@columbia.edu

J. N. Bruce
Department of Neurosurgery, College of Physicians and Surgeons of Columbia University, New York, NY 10032, USA

R. L. Fine
Division of Medical Oncology, Department of Internal Medicine, College of Physicians and Surgeons of Columbia University, New York, NY 10032, USA

assessed radiologically after the drugs have been delivered [6–9]. The ability to rapidly assess BBB integrity preferably in real-time could help optimize delivery of chemotherapeutic drugs that require such disruption by altering the dose of mannitol or the chemotherapeutic drugs based on the degree of BBB disruption. We therefore investigated whether brain uptake of ICG was affected by the disruption of the BBB.

In the present experiment, brain tissue concentrations of ICG were measured by using a novel optical technique called optical pharmacokinetics (OP) that uses diffuse reflectance spectroscopy [10–12]. The optical absorption spectrum of ICG in water and other solvents has a peak which is distinct from oxy- and deoxy-hemoglobin, Fig. 1. This facilitates the measurement of tissue concentrations of ICG by optical methods. We evaluated the changes in tissue concentration of ICG after an intravenous injection of the tracer before and after the hyperosmotic disruption of the BBB with intraarterial injection of mannitol in New Zealand white rabbits.

Materials and methods

Animal preparation

After approval of the investigation protocol by the Institutional Animal Care and Use Committees of Columbia University, studies were conducted on New Zealand white rabbits 1.5–2 kg in weight. The large size of their skull is convenient for implanting laser Doppler (LD) or placing OP probes for CBF and drug measurements, respectively. Rabbits have a primate like separation of internal and external carotid irrigations; therefore, they are well suited for

intraarterial drug delivery experiments. After placement of an intravenous line, the animals were anesthetized with 0.2–0.5 ml boluses of intravenous 1% propofol (Diprivan®, Astra Zeneca, Willmington, DL). Subsequently, through a tracheotomy, the animals were ventilated by Harvard small animal ventilator, aimed to produce an end-tidal CO_2 of 37 ± 5 mm Hg. Anesthesia was maintained with continuous propofol infusion at a rate of 20–30 mg/h and supplemental intramuscular ketamine. Compared to volatile anesthetics, intravenous propofol anesthesia does not adversely affect BBB disruption [13]. The depth of anesthesia was carefully controlled by monitoring the EEG pattern that in rabbits is characterized by an equal mix of high amplitude-low frequency waves superimposed on higher frequency-low amplitude rhythms [14]. An esophageal temperature probe monitored the core temperature of the animal. The animals were kept warm using a servo controlled electrical mattress. Femoral and common carotid arteries were cannulated. The internal carotid artery was carefully identified and isolated from other branches [15]. All other branches of the carotid artery were isolated and ligated. Isolation of internal carotid artery was confirmed by the intracarotid injection of saline (0.52–0.5 ml) bolus that resulted in transient retinal blanching [16].

Thereafter, the animals were placed prone in a stereotactic frame for the placement of electroencephalographic (EEG) leads, LD and OP probes. Through a midline incision, the periosteum of the skull was exposed. EEG leads were secured to the skull with 1.5 mm stainless steel screws. The skull was gently milled down, such that cerebral arteries could be seen through the inner table, in effect serving like a cranial window. The cranial vault integrity was not internally compromised. The LD probes were secured in plastic retainers that were glued to the skull.
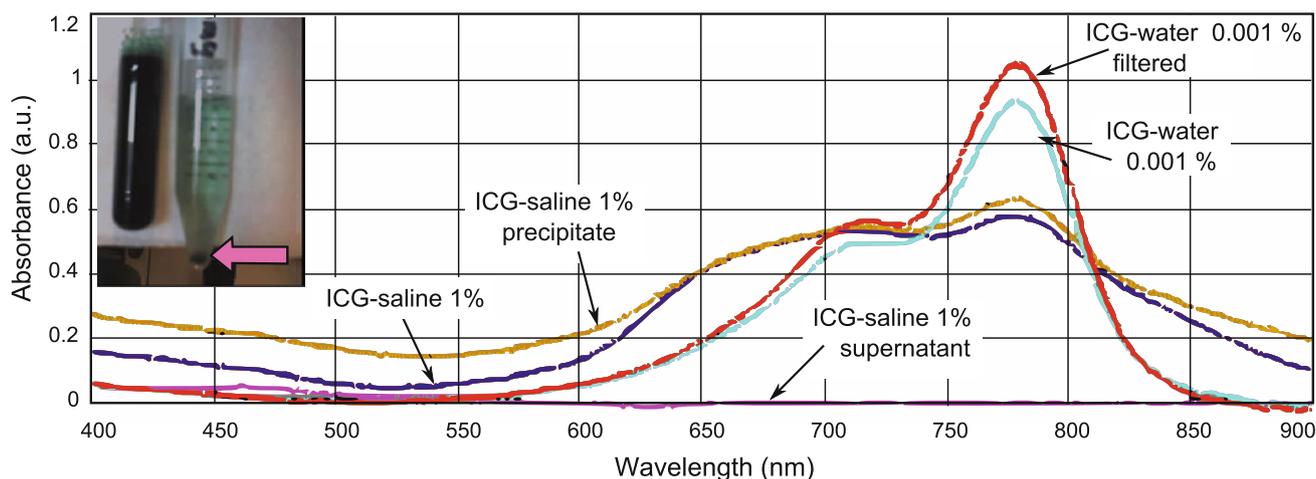

Fig. 1 ICG absorption spectrum: *Inset* ICG is freely soluble in water but not in saline in which it precipitates (*pink arrow*). In water, ICG produces a characteristic spectrum with peak absorbance at 780 nm that is minimally affected by filtration. In contrast, the ICG precipitates easily in saline and there is little light absorption by the supernatant

The OP probe was placed with a Kite micro-manipulator so that the probe tip was in gentle contact with the thinned skull over the brain, gently flattening the thinned bone. The OP probe has an external diameter of 3 mm, and was located so as to avoid placement over visible surface vessels; the baseline spectrum checked to ensure that the absorption of light in the hemoglobin region of the spectrum was not excessive. Meticulous care was taken to avoid any bleeding. Paper drains were placed around the surgical site to divert blood away from the site of OP measurements so as to avoid any contamination of the measurement site during the experiments. Bilateral hemispheric electrocerebral, and electrocardiographic activities, mean femoral arterial pressure, heart rate, CBF using LD, esophageal and tympanic temperatures, pulse oxygen saturation and the ventilatory parameters were recorded by Mac-Lab data (AD Instruments) collection system.

Optical pharmacokinetics

The method of *Optical Pharmacokinetics* is a version of diffuse reflectance spectroscopy, which enables the noninvasive real-time measurement of drug concentrations in situ. A schematic of the set-up and the abbreviated description of the method are provided in Fig. 2 [10–12]. The OP method estimates drug concentrations by measurement of the wavelength-dependent optical absorption coefficient of the tissue, and can be used for drugs that have an absorption band within the wavelength range from visible to near-infrared (450–950 nm). An optical fiber probe, comprising separate illumination and collection fibers, was placed in gentle contact with the tissue surface. Although the device can sample light backscattered from the subsurface tissue as frequently as every 50 ms, for the current study, the samples were acquired every 500–5,000 ms. The underlying optical-physics concepts for the OP method have been described in detail in earlier publications by Bigio et al. [10, 17, 19, 20], who have reported the preclinical measurements of chemotherapeutic drug concentrations in animal models in the peripheral tissues. It was shown that for an appropriate range of fiber separations, D, between light delivery and collection fibers, the pathlength of the collected photons, is insensitive to variations in scattering properties for the range of scattering parameters typically found in tissue. As employed in these studies, the fiber separation is 2 mm, and the depth of sensitivity is 2–3 mm [17].

The optical data was acquired at three different repetition rates with each ICG injection. Twelve baseline measurements were acquired at every 5,000 ms. Next, at the start of IV ICG injection, 300 measurements were acquired at 500 ms intervals to record the rapid first pass kinetics of the tracer through brain tissue. Finally, 300 measurements
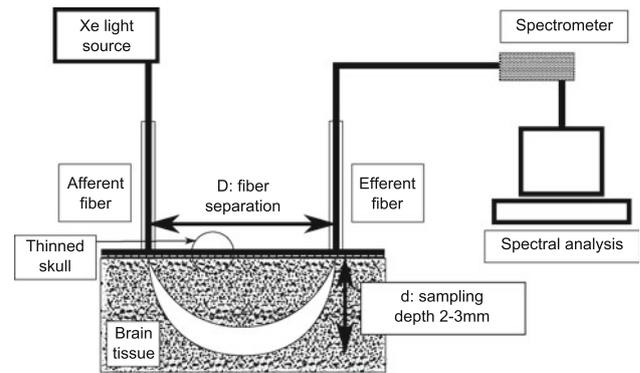

Fig. 2 Set-up for the optical pharmacokinetic device that uses a variation of diffuse reflectance spectroscopy for measuring concentrations of absorbers in turbid media

were collected at 5,000 ms intervals to record slower changes over a longer time period of about 40 min. Determination of ICG concentration is done by using a modified Beer's law from measurements collected before and after ICG administration. There were 612 data points for each ICG concentration-time curve. All computational analysis were completed using Matlab® (The MathWorks, Inc.) software.

ICG dose

Indocyanine green was selected as the optical tracer based on several reasons: ICG has an absorption spectrum that is distinct form hemoglobin and oxyhemoglobin. Its concentrations can be measured by both absorbance and fluorescence spectroscopy. ICG has been used for the determination of cerebral blood flow in humans and is approved for human diagnostic applications.

A 2.5% solution (by weight) of ICG (Cardio Green, Sigma Aldridge Co., St Louis MO) was prepared in sterile water immediately prior to use. The pH of the 2.5% ICG solution was 7.34. In a preliminary animal study, we determined the dose of ICG that would be rapidly cleared after IV administration and whose concentrations could be robustly measured by the OP method. We tested three doses 2.5, 10 and 20 mg. At the lowest dose, ICG concentration rapidly returned to zero, whereas residual ICG concentrations were seen with 10 and 20 mg doses at the end of 5 min, Fig. 3. We chose a dose of 7.5 mg for further experiments as it would not only be cleared rapidly yet it will generate optimum signal to noise ratio for optical measurements. To create a standard bolus input function, a pneumatic pump capable of injecting 3 ml of 0.25% IC in 2 s was used. We observed that all ICG signal was eliminated by 45 min after administering 7.5 mg dose before mannitol administration.
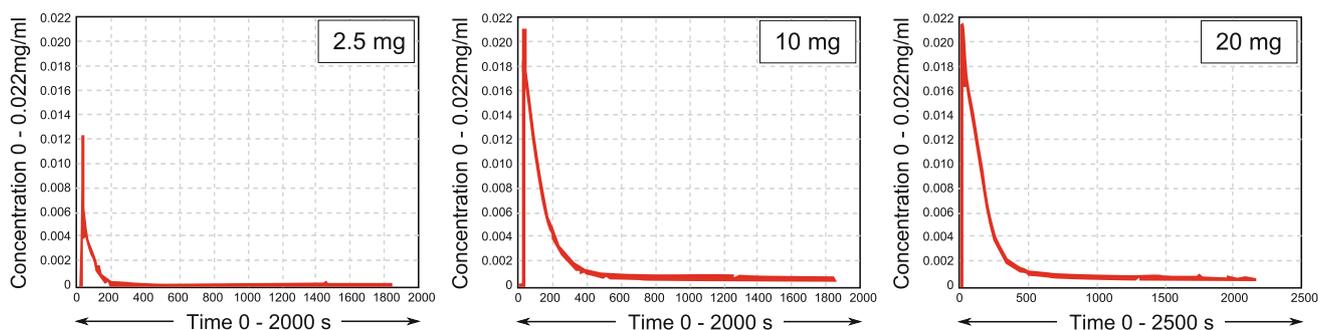
Fig. 3 Preliminary dose response study showing increase in brain tissue ICG concentrations with increasing total doses of ICG injected intravenously

Determination of tissue ICG concentrations

One of the challenges in this study was to determine the concentration of ICG in the brain tissue. As shown in Fig. 1, ICG absorption spectrum is affected by the solvent and the dye concentration. Furthermore, binding to blood plasma proteins causes changes in the absorption spectrum of ICG [21]. In our analysis, we determined the change in the absorption of the tissue due to the presence of ICG. We used a fitting algorithm to fit the experimental spectral data to the theoretical curves of ICG in addition to oxyhemoglobin and deoxy-hemoglobin to estimate the concentration of ICG in the brain tissue. After observing the spectral stabilization of ICG our raw spectral data, we chose to use a spectrum of ICG in plasma measured by Landsman et al. [21] as our theoretical curve which is more relevant for IV administration of this dye.
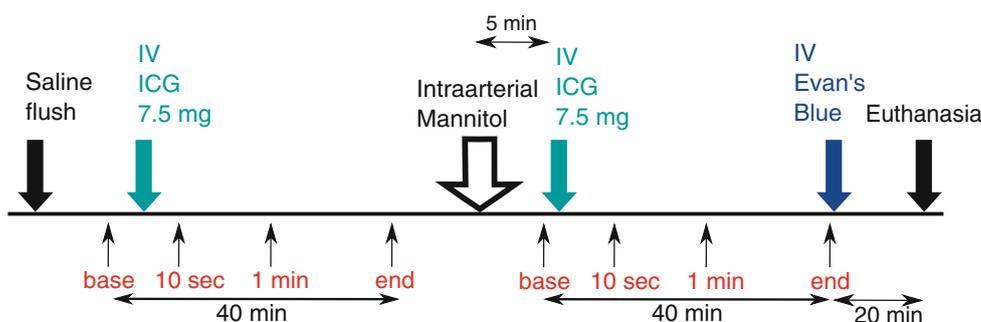
Experimental design

In parallel studies, we have observed that BBB disruption with intraarterial mannitol was highly variable in the rabbits [22]. Similar variability in the degree of BBB disruption has also been reported in human subjects [7]. Thus, the experimental protocol was designed to provide two types of comparisons regarding change in the brain tissue concentrations after ICG administration: The first, pre mannitol versus post mannitol; and the second, between animals that do or do not demonstrate the disruption of

BBB after mannitol treatment, at the site of OP measurements. The experimental protocol is shown in Fig. 4. The BBB was disrupted using 8 ml of 25% mannitol that was warmed and filtered immediately prior to injection. This dose was based on our own experience and that of other investigators [16, 22]. Human doses of mannitol are determined by the volume of tissue perfused and range between 90–400 ml over 30 s. Based on the rabbit brain weight of 10 gm and a blood flow of 100 ml/100 g/min, we estimate that 8 ml/30 s dose of mannitol, was equivalent to clinical doses used in humans. Mannitol was hand-injected over 30 s since the pump pressure required for the experiment was not within the pressure range of the standard mechanical pump available but meticulous care was taken to standardize the size and the duration of each bolus injection. At the end of the experiment, a saline solution of Evan's blue (50 mg/kg) was injected intravenously, and the animals were sacrificed 20 min later with an overdose of propofol (30 mg) and potassium chloride. The brain tissue was examined to determine the pattern Evan's blue staining specifically at the site of OP probe placement.

Data collection and analysis

The main outcome parameter in this study was the tissue concentrations of ICG. ICG concentration-time curve parameters that were analyzed included: (i) peak concentration (ii) immediate post injection concentrations at 10 s and 1 min after (iii) final brain tissue concentration at 40 min

Fig. 4 Drug delivery protocol: intravenous ICG was injected before and after intraarterial injection of mannitol

after ICG injection (iv) area under the concentration-time curve. The hemodynamic data for analysis included the heart rate, mean arterial pressure (MAP), CBF, core temperature, respiratory rate, end-tidal carbon-dioxide tension. Hemodynamic data were collected in real-time but were analyzed at six specific time points: (i) baseline, (ii) peak ICG, (iii) 30 s post ICG peak (iv) 5 min; (v) 15 min and (vi) at the end approximately 40 min after ICG injection.

Statistical data analysis

The data were analyzed by factorial and repeated measures ANOVA. For single factor comparisons, e.g., before and after mannitol and disrupted versus intact BBB, a P value of 0.05 was considered significant. Bonoferroni-Dunn test was used to correct for multiple comparisons among the hemodynamic parameters at six different stages of ICG injection. A P value of 0.0033 was considered significant for multiple comparisons of hemodynamic data.

Results

Hemodynamic response

Experiments were conducted on 13 New Zealand white rabbits with a mean weight of 1.7 ± 0.4 kg, $n = 13$. On post mortem examination of brain tissue, five of the 13 rabbits demonstrated no disruption of the BBB as

evidenced by a complete absence of Evan's blue staining. In another three rabbits, Evan's blue staining was evident (qualitatively) in areas of the brain that were not coincident with the site of OP measurements. The data from these eight animals was combined into a single group (BBB intact group) because the primary goal of this study was to determine if there was any retention of ICG when the BBB was disrupted at the site of OP measurements. Data from the animals that showed disruption of the BBB, as evidenced by Evan's blue staining, was combined into the BBB disrupted group, $n = 5$.

Pre and post mannitol comparisons

In both the pre and the post mannitol measurements, there was a transient decrease in CBF as measured by laser Doppler technique during ICG injection. The blood flow recovered within 5 min. The decrease in the laser Doppler CBF values was accompanied by a decrease in pulse oxygen saturation. Similar to the CBF decrease, the pulse oxygen saturation values also recovered within 5 min. The EEG remained unchanged before and after the injection of ICG. Collectively the pre and post mannitol changes in other physiological parameters were comparable, Table 1.

Effect of BBB disruption

There was no difference in the weights of the animals with ($n = 5$) or without BBB disruption ($n = 8$), 1.7 ± 0.4 kg in

Table 1 Changes in physiological parameters during ICG injection before and after mannitol injection in all animals ($n = 13$)

	Treatment	Baseline	Peak	30 s	5 min	15 min	40 min
Esophageal temperature (°C)	Pre mannitol	37.0 ± 1.1	36.9 ± 1.0	37.0 ± 1.0	37.1 ± 1.0	37.2 ± 0.9	37.2 ± 1.1
	Post mannitol	37.3 ± 0.8	37.3 ± 0.7	37.2 ± 0.8	37.3 ± 0.7	37.4 ± 0.7	37.5 ± 0.8
ETCO$_2$ (mm Hg)	Pre mannitol	38 ± 7	38 ± 7	38 ± 7	38 ± 7	38 ± 7	39 ± 7
	Post mannitol	39 ± 6	39 ± 6	39 ± 6	39 ± 6	39 ± 6	39 ± 6
Respiration rate (bpm)	Pre mannitol	45 ± 7	45 ± 7	45 ± 7	45 ± 7	45 ± 7	45 ± 7
	Post mannitol	45 ± 7	45 ± 7	45 ± 7	45 ± 7	45 ± 7	45 ± 7
SaO2 (%)	Pre mannitol	98 ± 5	80 ± 7[a]	85 ± 7[a]	94 ± 8	96 ± 4	97 ± 4
	Post mannitol	97 ± 5	82 ± 8[a]	88 ± 6[a]	94 ± 7	96 ± 5	97 ± 6
CBF (% change)	Pre mannitol	100 ± 0	44 ± 25[a]	69 ± 17	82 ± 29	91 ± 33	108 ± 33[c]
	Post mannitol	100 ± 0	40 ± 17[a]	67 ± 17	77 ± 17	77 ± 25	122 ± 25[c]
HR (bpm)	Pre mannitol	279 ± 21	270 ± 28	281 ± 22	282 ± 18	286 ± 18	287 ± 20
	Post mannitol	279 ± 20	274 ± 24	281 ± 17	281 ± 22	282 ± 26	285 ± 16
MAP (mmHg)	Pre mannitol	88 ± 21	82 ± 25	88 ± 19	92 ± 22	91 ± 25	92 ± 25
	Post mannitol	94 ± 24[b]	93 ± 18[b]	99 ± 21	92 ± 21	81 ± 22	78 ± 21

The data is presented as mean $\pm$ 1 standard deviations

BPM breaths/min, *CBF* CBF as measured by laser Doppler and expressed as %-change from baseline, *SaO$_2$* arterial blood oxygen saturation

[a] Different from baseline and other stages of the experiment

[b] Different from 30 s

[c] Different from 5 min

Table 2 Physiological changes in post mannitol ICG injection animals with BBB disruption (BBB−, n = 5) and without (BBB+, n = 8)

	BBB±	Baseline	Peak	30 s	5 min	15 min	40 min
Temperature (°C)	BBB+	37.5 ± 0.9	36.4 ± 0.6	37.5 ± 0.7	37.5 ± 0.6	37.6 ± 0.8	37.9 ± 0.8
	BBB −	37.1 ± 0.8	37.1 ± 0.9	37.0 ± 0.8	36.9 ± 0.6	37.1 ± 0.7	36.9 ± 0.6[d]
ETC0$_2$ (mm Hg)	BBB+	38 ± 7	38 ± 7	38 ± 7	38 ± 7	38 ± 7	38 ± 7
	BBB−	40 ± 6	40 ± 5	39 ± 4	40 ± 5	41 ± 7	41 ± 7
RR (bpm)	BBB+	45 ± 5	45 ± 5	45 ± 5	45 ± 5	45 ± 5	45 ± 5
	BBB−	47 ± 9	47 ± 9	47 ± 9	47 ± 9	47 ± 9	47 ± 9
Sa02 (%)	BBB+	97 ± 7	81 ± 8[a]	88 ± 6[a]	92 ± 7	95 ± 5	96 ± 8
	BBB−	99 ± 2	85 ± 7[a]	89 ± 7[a]	97 ± 5	98 ± 2	98 ± 3
CBF (% change)	BBB+	100 ± 0	41 ± 20[a]	69 ± 21[a]	76 ± 18[b]	79 ± 22[b,c]	120 ± 22[b,c]
	BBB−	100 ± 0	39 ± 10[a]	65 ± 15	79 ± 18	74 ± 33	125 ± 33[b,c]
HR (bpm)	BBB+	288 ± 18	287 ± 16	291 ± 12	295 ± 11	296 ± 12	291 ± 11
	BBB−	264 ± 13	254 ± 20	266 ± 14	258 ± 15	261 ± 20	276 ± 21
MAP (mm Hg)	BBB+	92 ± 28	91 ± 24	98 ± 26	89 ± 24	82 ± 27[b]	78 ± 27[b]
	BBB−	96 ± 16	95 ± 9	100 ± 12	96 ± 16	79 ± 14	78 ± 12

The data is presented as mean ± 1 standard deviations

BPM breaths/min, *CBF* cerebral blood flow as measured by laser Doppler and expressed as %-change from baseline, *SaO$_2$* arterial blood oxygen saturation

[a] Different from base

[b] Different from peak

[c] Different from 30 s

[d] Different between groups

both groups. Direct comparison of the BBB-intact and BBB-disrupted groups revealed that the systemic hemodynamic responses were identical in the two groups except for the difference in temperature at the end of the experiment, 36.9 ± 0.6°C in animals with a disrupted BBB versus 37.9 ± 0.8°C in animals with intact BBB (P = 0.045). The baseline temperature was comparable between the two groups 37.1 ± 0.8 versus 37.5 ± 0.9°C, respectively. In animals with BBB disruption, a slight decrease in MAP was seen towards the end of the experiment with no concurrent decline in CBF, Table 2.

Tissue ICG concentrations

For the whole group, the peak concentrations of ICG were comparable before and after the injection of mannitol 304 ± 103 versus 321 ± 121 µg/g, respectively, n = 13, P = NS. The area under the ICG concentration time curve [0–40 min] showed a trend towards a statistically significant increase after mannitol injection 18.8 ± 7.1–36.8 ± 31.2 mg/g s, n = 13, P = 0.053. The concentrations of ICG at the end of 40 min increased after BBB disruption, pre versus post mannitol, from 2 ± 1 to 9 ± 10 µg/g, n = 13, P = 0.041, Fig. 5–6.

However when the animals were segregated into those with BBB disruption (n = 5) at the site of optical measurements and those without (n = 8), a much greater difference was evident between the two groups. The pre and post mannitol peak ICG concentrations were not statistically different in those with or without BBB disruption, see Table 3. However, the area under the ICG concentration-time curve was fourfold greater in animals with disrupted BBB post mannitol injection, compared to those without BBB disruption, 18.1 ± 7.2 versus 64.6 ± 36 mg/g s, P = 0.03. The concentration of ICG at the end of 40 min increased ninefold, 2 ± 1 versus 18 ± 10 µg/g, P < 0.03, Fig. 6. These results show considerable individual variation but collectively significant retention of ICG after BBB disruption.

Discussion

The results of our experiments show subtle yet significant retention of ICG after the disruption of the BBB. We observed that post mortem Evan's blue staining varied considerably among animals in terms of the intensity and distribution of BBB disruption after intraarterial injection of hypertonic mannitol. Across all 13 animals, the brain tissue concentrations of ICG and the area under the ICG concentration-time curve showed a trend towards an increase that was not statistically significant due to large individual variability. However, when the animals were separated into two groups based on BBB disruption at the
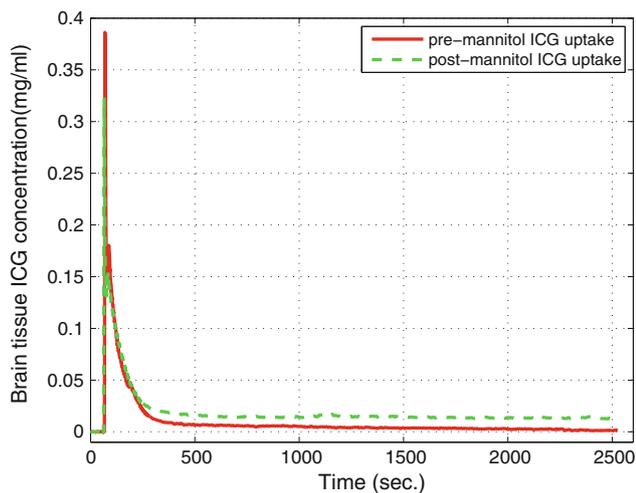
Fig. 5 Optically measured brain tissue concentrations of ICG before and after the disruption of BBB

site of optical measurements, the tissue concentrations of ICG at the 40-min time point in the BBB disruption group were ninefold higher, and the area under the concentration-time curve was fourfold greater, as compared to the animals without BBB disruption.

Before discussing the implications of the results, we wish to address methodological concerns. First, we assessed the BBB disruption with Evan's blue injection approximately 45 min after mannitol injection. The molecular weights of Evan's blue and ICG are 960 and 775 Daltons, respectively. Although both are bound to albumin (mol. wt. 68,000 Dalton), they dissociate and can be taken up by the brain tissue when the BBB is disrupted. Traditionally Evan's blue uptake is a marker for BBB disruption. We delayed the injection of Evan's blue because the dose of Evan's blue required to demonstrate the disruption of the BBB is so large (50 mg/kg) that it makes it difficult to accurately determine the trace levels of ICG concentration that are

retained by the brain tissue. While some believe that hyperosmotic BBB disruption with mannitol is transient, other studies show that BBB may remain disrupted for several hours after mannitol injection [23]. In clinical settings, BBB disruption is often assessed 60–90 min after mannitol injection [8]. Our own observations suggest that the disruption of BBB after mannitol is usually sustained for at least an hour afterwards. Therefore, we believe that Evan's blue staining provided a reliable indicator of BBB disruption at the site of optical measurements despite the delayed injection of the dye [22].

Second, the geometry of our probe was designed to sample a fairly small volume of tissue and in three animals failed to report the disruption of the BBB that occurred remote from the site of measurements. We have since designed other probes that interrogate a bigger region of interest although the depth of the measurement remains the same between 2 and 2.5 mm. The small probe size, resulting in a small volume that is sensed, was necessitated by the small volume of the rabbit brain relative to the skull and scalp thickness. However even a larger probe would not have been able to reveal remote disruptions such as in the posterior circulation that was seen in these animals by Evan's blue staining.

Our interest in ICG as a marker of BBB disruption arises due to several reasons. First, ICG is a valuable tracer for a number of physiological and diagnostic studies and is approved for a variety of human uses [1–3, 24]. Second, ICG concentrations in the brain tissue of human subjects can be measured by modification of commercially available noninvasive NIRS technology [4]. Third, ICG is rapidly cleared from the systemic circulation by the liver and has a very short biological half-life, which could permit repeat assessments of BBB integrity [25]. Finally, in vivo studies have assessed the safety of ICG with concurrent NIRS measurements in the settings of BBB disruption [26].

Table 3 Changes in optically measured ICG concentrations before and after injection of intraarterial mannitol

	Condition	All animals (n = 13)	BBB intact (n = 8)	BBB disrupted (n = 5)
Peak concentration (μg/ml)	Pre mannitol	304 ± 103	281 ± 121	341 ± 59
	Post mannitol	321 ± 121	281 ± 112	386 ± 118
10 s Post injection (μg/ml)	Pre mannitol	116 ± 49	103 ± 33	137 ± 67
	Post mannitol	127 ± 52	106 ± 30	161 ± 64
1 min post injection (μg/ml)	Pre mannitol	66 ± 29	63 ± 30	70 ± 30
	Post mannitol	86 ± 47	67 ± 20	116 ± 63
End concentration (μg/ml)	Pre mannitol	2 ± 1	2 ± 2	2 ± 1
	Post mannitol	9 ± 10[a]	2 ± 1	18 ± 10[a]
AUC (mg/ml-s)	Pre mannitol	18.8 ± 7.1	19.3 ±±7.5	18.1 ± 7.2
	Post mannitol	36.8 ± 31	19.5 ± 5	64.6 ± 36[a,b]

[a] Different from Pre-mannitol $P < 0.05$

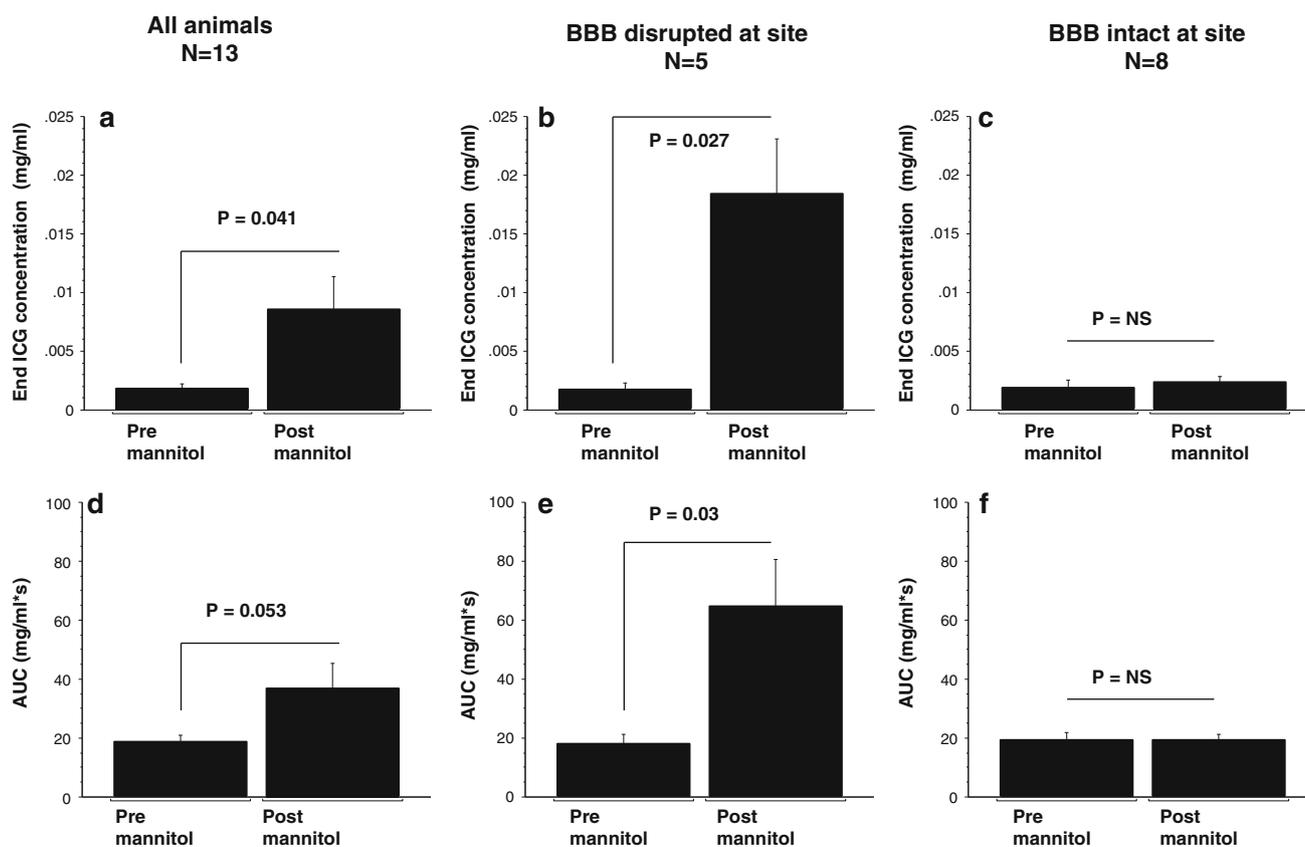[b] Different between BBB intact and disrupted groups

Fig. 6 *Bar charts* showing optically measured brain tissue ICG concentrations before and after intraarterial mannitol injections. **a**–**c** Show the end concentration of ICG while **d**–**f** show the area under the concentration-time curve in all animals, $n = 13$ (**a**, **d**); in those that had no postmortem Evan's blue staining, $n = 8$ (**c**, **f**); and those that had positive Evan's blue staining at the site of ICG measurements, $n = 5$ (**b**, **e**)

Although it is often assumed that ICG will diffuse across a disrupted BBB, the evidence regarding the actual deposition of the dye in the brain tissue after BBB disruption is inconsistent. In an embolic model of BBB disruption, ICG has been shown to leak across the BBB some 3–5 min after injection [27]. In contrast, a rat model using intraarterial mannitol for the disruption of the BBB, failed to demonstrate a significant increase in ICG concentrations [26]. As in the present study, BBB disruption in the latter study could be demonstrated by post mortem Evan's blue staining. A number of factors affect BBB disruption by hypertonic agents, and these include regional variability [13]. Variations in the intensity and distribution of BBB disruption after intraarterial mannitol could greatly affect the outcome of chemotherapeutic studies. Optical techniques often measure concentrations in a small volume of tissue and could therefore result in sampling errors.

Measurement of ICG concentrations in the brain can be done by several optical means. Of special note are advancements in near-infrared spectroscopy of deeper brain tissues (up to ~5 cm) as a result of development of methods for diffuse optical tomography [28–30]. Spatial separation of the afferent and efferent fibers is widely used in cerebral oximetry. Commercially available cerebral oximeter have been used to measure ICG concentrations in the human brain tissue [26]. Recently, time-resolved approaches have also been used in tissue phantoms to determine tissue ICG concentrations [31]. Time-resolved approaches have also been successfully used, with optical grid arrangements, for topographical mapping of human CBF changes [32, 33]. Such grid arrangements could help in tracking ICG concentrations and permeability changes over larger tumor surfaces.

Yet, the variability of BBB disruption with intraarterial mannitol is precisely the reason why we are interested in investigating the uptake of ICG after BBB disruption. Several neuropharmaceuticals, native drugs, their liposomal formulations and even viral vectors require disruption of the BBB to improve drug delivery, particularly for intraarterial administration [34]. Despite several encouraging alternative developments, hypertonic mannitol remains the primary means of disrupting the BBB after three decades of use [6]. Limited human data clearly show a considerable variability (tenfold) in BBB disruption after

mannitol along with a 25-fold variation in CSF chemo-therapeutic drug concentrations [7]. Although rare, significant complications do occur during BBB disruption procedures [8, 9]. Thus, there is a clinical need to rapidly assess the state of BBB permeability or extent of BBB disruption after intraarterial mannitol. Histological specimen of rats with implanted glioma cells show ICG staining of the tumor edge, [35]. If tumor tissue permeability is detected before hand it would avoid the need for intraarterial mannitol to disrupt the BBB. Furthermore rapid assessment of blood-tumor barrier before chemotherapy might obviate the need to disrupt the BBB.

The current intraarterial BBB disruption technique often requires a radiological assessment of BBB disruption [7–9]. Such a test involves the injection of radiocontrast, which is potentially neurotoxic; and for logistical reasons, it is often undertaken after chemotherapeutic drugs have been injected. A real-time optical assessment of BBB functions could help improve chemotherapy by assessing the need for disruption, optimizing the dose of mannitol or adjusting the dose of the chemotherapeutic drug based on the degree of BBB disruption. Optical methods of assessing BBB disruption could therefore help improve the outcome of intraarterial chemotherapy.

In conclusion, this experiment shows a significant uptake of ICG in brain tissue after osmotic disruption of BBB, concentrations of which can be optically monitored. These results should encourage refinement of NIRS technologies to track in vivo ICG concentrations through an intact human cranial vault, during clinical procedures. Ability to optically track tissue concentrations of tracers such as ICG that can detect, and perhaps quantify the extent of BBB disruption, will further enhance the safety of BBB disruption procedures. It could help to manage the dose of mannitol and/or chemotherapeutic drug based on the degree of BBB disruption.

References

1. Windisch R, Windisch BK, Cruess AF (2008) Use of fluorescein and indocyanine green angiography in polypoidal choroidal vasculopathy patients following photodynamic therapy. Can J Ophthalmol 43:678–682

2. Simon R, Desebbe O, Henaine R et al (2009) Comparison of ICG thoracic bioimpedance cardiac output monitoring system in patients undergoing cardiac surgery with pulmonary artery cardiac output measurements. Ann Fr Anesth Reanim 28:537–541

3. Dashti R, Laakso A, Niemela M et al (2010) Application of microscope integrated indocyanine green video-angiography during microneurosurgical treatment of intracranial aneurysms: a review. Acta Neurochir Suppl 107:107–109

4. Keller E, Nadler A, Alkadhi H et al (2003) Noninvasive measurement of regional cerebral blood flow and regional cerebral blood volume by near-infrared spectroscopy and indocyanine green dye dilution. Neuroimage 20:828–839

5. Schytz HW, Wienecke T, Jensen LT et al (2009) Changes in cerebral blood flow after acetazolamide: an experimental study comparing near-infrared spectroscopy and SPECT. Eur J Neurol 16:461–467

6. Neuwelt E, Abbott NJ, Abrey L et al (2008) Strategies to advance translational research into brain barriers. Lancet Neurol 7:84–96

7. Zylber-Katz E, Gomori JM, Schwartz A et al (2000) Pharmacokinetics of methotrexate in cerebrospinal fluid and serum after osmotic blood–brain barrier disruption in patients with brain lymphoma. Clin Pharmacol Ther 67:631–641

8. Marchi N, Angelov L, Masaryk T et al (2007) Seizure-promoting effect of blood–brain barrier disruption. Epilepsia 48:732–742

9. Elkassabany NM, Bhatia J, Deogaonkar A et al (2008) Perioperative complications of blood–brain barrier disruption under general anesthesia: a retrospective review. J Neurosurg Anesthesiol 20:45–48

10. Mourant JR, Johnson TM, Los G, Bigio IJ (1999) Non-invasive measurement of chemotherapy drug concentrations in tissue: preliminary demonstrations of in vivo measurements. Phys Med Biol 44:1397–1417

11. Bigio IJ, Bown SG (2004) Spectroscopic sensing of cancer and cancer therapy: current status of translational research. Cancer Biol Ther 3:259–267

12. Reif R, Wang M, Joshi S et al (2007) Optical method for real-time monitoring of drug concentrations facilitates the development of novel methods for drug delivery to brain tissue. J Biomed Opt 12:034–036

13. Remsen LG, Pagel MA, McCormick CI et al (1999) The influence of anesthetic choice, PaCO2, and other factors on osmotic blood–brain barrier disruption in rats with brain tumor xenografts. Anesth Analg 88:559–567

14. Joshi S, Wang M, Etu JJ, Pile-Spellman J (2005) Reducing cerebral blood flow increases the duration of electroencephalographic silence by intracarotid thiopental. Anesth Analg 101:851–858 Table of contents

15. Joshi S, Wang M, Hartl R (2004) Retinal discoloration test. J Cereb Blood Flow Metab 24:305–308

16. Perkins BA, Strausbaugh LJ (1983) Effect of mannitol infusions into the internal carotid artery on entry of two antibiotics into the cerebrospinal fluid and brains of normal rabbits. Antimicrob Agents Chemother 24:339–342

17. Bigio IJ, Mourant JR, Los G (1999) Noninvasive, in situ measurement of drug concentrations in tissue using optical spectroscopy. J Gravit Physiol 6:P173–P175

18. Kanick SC, Eiseman JL, Joseph E et al (2007) Noninvasive and nondestructive optical spectroscopic measurement of motexafin gadolinium in mouse tissues: comparison to high-performance liquid chromatography. J Photochem Photobiol B 88:90–104

19. Mourant JR, Bigio IJ, Jack DA, Johnson DM, Miller HD (1997) Measuring absorption coefficients in small volumes of highly scattering media: source-detector separations for which pathlengths do not depend on scattering properties. Appl Optics 36(22):5655–5661

20. Bigio IJ, Mourant JR (1997) Ultraviolet and visible spectroscopies for tissue diagnostics: fluorescence spectroscopy and elastic-scattering spectroscopy. Phys Med Biol 42:803–814

21. Landsman ML, Kwant G, Mook GA, Zijlstra WG (1976) Light-absorbing properties, stability, and spectral stabilization of indocyanine green. J Appl Physiol 40:575–583

22. Wang M, Etu J, Joshi S (2007) Enhanced disruption of the blood–brain barrier by intracarotid mannitol injection during transient

cerebral hypoperfusion in rabbits. J Neurosurg Anesthesiol 19:249–256

23. Bellavance MA, Blanchette M, Fortin D (2008) Recent advances in blood–brain barrier disruption as a CNS delivery strategy. AAPS J 10:166–177

24. Deja M, Ahlers O, Macguill M et al (2010) Changes in hepatic blood flow during whole body hyperthermia. Int J Hyperthermia 26:95–100

25. Geneve J, Le Dinh T, Brouard A et al (1990) Changes in indocyanine green kinetics after the administration of enalapril to healthy subjects. Br J Clin Pharmacol 30:297–300

26. Keller E, Ishihara H, Nadler A et al (2002) Evaluation of brain toxicity following near infrared light exposure after indocyanine green dye injection. J Neurosci Methods 117:23–31

27. Kim DE, Schellingerhout D, Jaffer FA et al (2005) Near-infrared fluorescent imaging of cerebral thrombi and blood–brain barrier disruption in a mouse model of cerebral venous sinus thrombosis. J Cereb Blood Flow Metab 25:226–233

28. McCormick PW, Stewart M, Lewis G et al (1992) Intracerebral penetration of infrared light. Technical note. J Neurosurg 76:315–318

29. Gratton E, Fantini S, Franceschini MA et al (1997) Measurements of scattering and absorption changes in muscle and brain. Philos Trans R Soc Lond B Biol Sci 352:727–735

30. Chance B, Leigh JS, Miyake H et al (1988) Comparison of time-resolved and -unresolved measurements of deoxy-hemoglobin in brain. Proc Natl Acad Sci USA 85:4971–4975

31. Liebert A, Wabnitz H, Steinbrink J et al (2004) Time-resolved multidistance near-infrared spectroscopy of the adult head: intracerebral and extracerebral absorption changes from moments of distribution of times of flight of photons. Appl Opt 43:3037–3047

32. Boas D, D FR (2005) Optics in neuroscience. J Biomed Opt 10:1–2

33. Koh PH, Glaser DE, Flandin G et al (2007) Functional optical signal analysis: a software tool for near-infrared spectroscopy data processing incorporating statistical parametric mapping. J Biomed Opt 12:064010

34. Joshi S, Meyers PM, Ornstein E (2008) Intracarotid delivery of drugs: the potential and the pitfalls. Anesthesiology 109:543–564

35. Kala M (1994) Indocyanine green (ICG) staining and demarcation of tumor margins in a rat glioma model. Surg Neurol 42:552–554